



Queensland University of Technology
Brisbane Australia

This is the author's version of a work that was submitted/accepted for publication in the following source:

Cheng, Hongfei, Liu, Qinfu, Zhang, Shuai, Wang, Shaoqing, & [Frost, Ray L.](#)

(2014)

Evolved gas analysis of coal-derived pyrite/marcasite.

Journal of Thermal Analysis and Calorimetry, 116(2), pp. 887-894.

This file was downloaded from: <http://eprints.qut.edu.au/83581/>

© Copyright 2014 Akademiai Kiado, Budapest, Hungary

Note: the archived file is an accepted manuscript, not the final published version of the paper, published version maybe viewed at publisher's website: <http://dx.doi.org/10.1007/s10973-013-3595-0>

Notice: *Changes introduced as a result of publishing processes such as copy-editing and formatting may not be reflected in this document. For a definitive version of this work, please refer to the published source:*

<http://dx.doi.org/10.1007/s10973-013-3595-0>

Evolved gas analysis of coal-derived pyrite/marcasite

Hongfei Cheng ^{a,b,c}, Qinfu Liu ^{a*}, Shuai Zhang ^a, Shaoqing Wang ^a, Ray L. Frost ^{c*}

^a School of Geoscience and Surveying Engineering, China University of Mining & Technology, Beijing 100083, P.R. China

^b State Key Laboratory of Coal Resources and Safe Mining, China University of Mining & Technology, Beijing 100083, P.R. China

^c School of Chemistry, Physics and Mechanical Engineering, Science and Engineering Faculty, Queensland University of Technology, 2 George Street, GPO Box 2434, Brisbane, Queensland 4001, Australia

Abstract

The products evolved during the thermal decomposition of the coal-derived pyrite/marcasite were studied by using simultaneous thermogravimetry coupled with Fourier-transform infrared spectroscopy and mass spectrometry (TG-FTIR-MS) technique. The main gases and volatile products released during the thermal decomposition of the coal-derived pyrite/marcasite are water (H₂O), carbon dioxide (CO₂), sulfur dioxide (SO₂). The results showed that the evolved products obtained were mainly divided into two processes: 1) the main evolved product H₂O is mainly released at below 300 °C; 2) under the temperature of 450-650 °C, the main evolved products are SO₂ and small amount of CO₂. It is worth mentioning that SO₃ was not observed as a product as no peak was observed in the m/Z=80 curve. The chemical substance SO₂ is present as the main gaseous product in the thermal decomposition for the sample. The coal-derived pyrite/marcasite is different from mineral pyrite in thermal decomposition temperature. The mass spectrometric analysis results are in good agreement with the infrared spectroscopic analysis the evolved gases. These results give the evidence on the thermal decomposition products and make all explanation have the sufficient evidence. Therefore, TG-MS-IR is a powerful tool for the investigation of gas evolution from the thermal decomposition of materials and its intercalation complexes.

Keywords: pyrite, marcasite, thermal decomposition, evolved gas, sulfur dioxide

* Corresponding authors. Fax: +86 10 62331825 (Q. Liu), +61 7 3138 2407 (R. L. Frost)
E-mail addresses: lqf@cumtb.edu.cn (Q. Liu), r.frost@qut.edu.au (R. L. Frost)

1 **Introduction**

2 Pyrite, with chemical formula FeS_2 , is a quite frequently occurred mineral of sulfur and
3 is found in a wide range of geological sites [1]. In nature, pyrite existed in the sulfur minerals
4 and coal in the fine dispersed case as well as in free forms [2-4]. Pyritic and organic sulfur are
5 the two major forms of sulfur in coal [5-9]. The wide occurrence of pyrite in different
6 minerals and coals makes it one of the main sources of SO_2 emission from various industrial
7 activities, such as the metallurgical industry, power production and cement production. It was
8 found that SO_2 is formed when pyrite is oxidized in industrial processes [10]. In countries
9 such as China, pyrite is very abundant and dominant sulfide compound in coal. Although it is
10 only composed of a relatively small portion of coal, it almost influences and decides the
11 operational, environmental and economic performance of handling and utilizing processes of
12 coal [11, 12]. It might be one of the most striking examples of how the reactivity of pyrite can
13 affect an environment is associated with anthropogenic activities. The oxidative
14 decomposition of pyrite in coal mining sites leads to the devastating environmental problem
15 known as acid mine drainage [13]. This is because pyrite releases a major source of SO_2 (acid
16 rain precursor) in the combustion process and many evidences also suggest that it may
17 possibly possess a catalytic role in coal liquefaction and gasification processes. Given the
18 environmental concerns pyrite oxidation presents, there has been an intense scientific effort to
19 understand the oxidation process and to develop methods to protect the pyrite surface from
20 the deleterious effects of oxidation [14].

21 Several researchers have studied the thermal decomposition of pyrite. Eneroth and Koch
22 [15] studied the thermal oxidation of pyrite and its polymorph, marcasite by heating pyrite

23 between 200 and 650 °C for 1 h in the presence of oxygen and reported hematite as the main
24 product. Sit et al.[16] reported that the adsorption and reactions of water and O₂ with the FeS₂
25 (100) surface provides detailed mechanistic insight into pyrite oxidation and the complex
26 electron flow accompanying this process. Oxidation of the pyrite surface occurs through
27 successive reactions of the surface with adsorbed O₂ and water molecules. The gaseous
28 degradation products seem also to be known for a long time from work of Hansen [17], who
29 mentioned measurable SO₂ formation are mainly caused by the oxidation of pyrite. However,
30 a evolved gas analysis (EGA) study [18] only use mass spectroscopic data to illustrate the
31 oxidation products by identifying their presence from the characteristic thermal
32 decomposition process, and the infrared spectroscopic analysis of evolved gaseous mixtures
33 from pyrite was not mentioned in this study. A more recent similar study [12] carried out
34 under inert atmosphere still contains some uncertainties in identification of the gaseous
35 species evolved by the temperature-programmed decomposition-mass spectrometer analysis.

36 In order to elucidate the basic reactions processes of thermal decomposition of pyrite in
37 oxidative atmosphere, here we present our study on identification and tracking of evolving
38 gaseous species from the coal-derived pyrite/marcasite pyrolysis using simultaneous
39 thermogravimetry coupled with Fourier-transform infrared spectroscopy and mass
40 spectrometry (TG-FTIR-MS). TG-FTIR-MS a powerful method has been used in previous
41 studies to measure evolved gases during the thermal treatment of various substances [6,19-22].
42 The components of released gaseous mixtures have been monitored and identified mostly on
43 the basis of their Fourier-transform infrared spectroscopy (FTIR) and mass spectrometry (MS).
44 Evolution curves obtained in flowing air by TG-MS-FTIR methods are compared in details

45 [23-25]. This method offers the potential for the non-destructive, simultaneous, real-time
46 measurement of multiple gas phase compounds in complex mixture.

47

48 **Experimental methods**

49 *Materials*

50 The coal-derived pyrite/marcasite sample used in the present investigation was extracted
51 from the Qinshui coalfield, Shanxi province of China. The initial sample of the coal-derived
52 pyrite/marcasite with particle size 0.1-0.2 mm was first subjected to gravity separation to
53 remove the inclusions of coal using a laboratory mechanical pan (Micropaner). Then, the
54 obtained concentrate was cleaned by means of magnetic separation. The mineral composition
55 of the final product was estimated by X-ray diffraction (XRD). The XRD pattern for the
56 coal-derived pyrite/marcasite is presented in Fig. 1.

57

58 *Characterization*

59 *X-ray diffraction (XRD)*

60 The XRD pattern of the prepared sample was performed by using a Rigaku D/max 2500PC
61 X-ray diffractometer with Cu ($\lambda=1.54178 \text{ \AA}$) irradiation at the scanning rate of $2^\circ/\text{min}$ in the
62 2θ range of $2.6-70^\circ$, operating at 40 kV and 150 mA.

63 *In situ TG-MS-FTIR*

64 The *in situ* TG-FTIR-MS analysis was performed using simultaneous thermogravimetry
65 (Netzsch Sta 449 C) coupled with FTIR (Bruker Tensor 27) and mass spectrometry
66 (ThermoStar, Pfeiffer Vacuum). About 10 mg of the sample was heated under air, a heating
67 rate of 5°C min^{-1} from 30°C to 800°C . The gas ionization was performed at 100 eV. The

68 m/z was carried out from 1 to 100 atomic mass units (amu) to determine which m/z has to be
69 followed during the TG experiments. The intensities of 11 selected ions (m/z = 15, 16, 17, 18,
70 32, 33, 34, 44, 48, 64 and 80) were monitored with the thermogravimetric parameters.
71 However, the ion curves close to the noise level were omitted. Finally, only the intensities of
72 9 selected ions (m/z = 16, 17, 18, 32, 34, 44, 48, 64 and 80) were discussed in mass
73 spectrometric analysis. The bottom of the thermoanalyser was heated to about 200 °C to
74 eliminate cold points in the connecting line. The FTIR spectra were collected at a resolution
75 of 4 cm⁻¹, and 200 scans were co-added per spectrum. The literature on the thermal
76 decomposition of pyrite shows that the most important gaseous products evolved during
77 devolatilisation are SO₂ and SO₃. Therefore, although some ionic species, in this study, were
78 produced during the pyrolysis, the following gaseous species were specially studied: CO₂,
79 H₂O, SO₂ and SO₃.

80

81 **Results and discussion**

82 *XRD results*

83 The XRD pattern of the sample together with standard XRD patterns is shown in Fig. 1,
84 which indicates that the sample contains mainly pyrite and marcasite. According to the
85 quantitative XRD analysis, the mineral composition of the sample is shown in Table 1.
86 Compared with the standard Joint Committee on Powder Diffraction Standards (JCPDS) cards,
87 the XRD pattern for the raw pyrite showed peak intensity at $2\theta=28.51, 33.08, 37.11, 40.78,$
88 $47.41, 50.49, 56.28$ which suggested a very high degree of purity according to JCPDS file
89 [12]. The crystallographic structure of pyrite as taken by the name-giving chemical compound

90 of composition FeS₂ was among the earliest structures solved by XRD procedures. It was
91 reported that the Fe ions build up a face-centered cubic lattice, into which the sulfur ions are
92 embedded. The space lattice resembles that of sodium chloride, with Fe²⁺ replacing the
93 sodium and S₂²⁻ replacing the chloride.

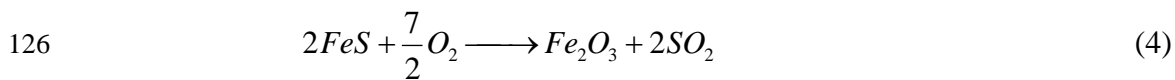
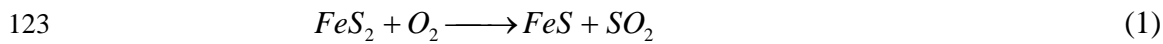
94 Pyrite has a cubic structure with lattice constant a=5.419 Å, which is consistent with the
95 previous literature [26]. Its space group is Pa3 with crystal cell molecules Z=4. The crystalline
96 size of the sample is about 20 nm, which is calculated from the XRD peaks using the
97 Scherrer's formula. Although the structure of pyrite cannot be classified as essentially close
98 packed, it is still a very dense material [27]. The four molecules in the unit cube are in special
99 positions T_h⁶ (Pa3). However, marcasite crystallizes in the orthorhombic system with a
100 distinctive structure, which, like pyrite, gives it a self-identified position in the structure
101 typology. Most of the data on marcasite and its isomorphs indicate a dimolecular unit, but
102 faint reflections have suggested a tetramolecular cell. The structure is less dense than pyrite.

103

104 *Thermal analysis*

105 A typical record of the thermogravimetry and derivative thermogravimetric (TG-DTG)
106 analysis curves of the coal-derived pyrite/marcasite is shown in Fig. 2. Six mass loss steps are
107 observed (a) from 85 to 140 °C (b) at 148 °C (c) between 210 and 300 °C with the maximum
108 rate at 251 °C (d) three consecutive mass losses between 450 and 650 °C corresponded to
109 mass losses of 12.34% (450-520 °C), 8.07% (520-575 °C) and 4.68% (575-650 °C). The main
110 reaction, as shown by both the TG and DTG curves, became apparent between 450 and
111 650 °C. According to the previous reports [18, 17, 28, 29], the thermal decomposition of

112 pyrite mainly occurs at 450-480 °C, 530-570 °C and 630-690 °C. The first mass loss of 4.76%
113 is attributed to loss of the adsorbed water. The second mass loss of 2.36% is assigned to the
114 loss of interparticle water for the sample. The third mass loss of 4.6% between 200 and
115 300 °C with a maximum at 251 °C is due to the evolution of sulfur on the pyrite surface and
116 loss of the rest part of interparticle water. Yan et al. [12] reported that the existence of
117 elemental sulfur at pyrite surface have also been confirmed by other authors using Raman
118 spectroscopy and X-ray photoelectron spectroscopy analysis. Three higher temperature
119 decomposition steps are observed at 501, 548 and 598 °C with mass losses of 12.34, 8.07 and
120 4.68% making a total mass loss at these temperatures of 25.09%. In these three temperature
121 steps SO₂ is evolved which was confirmed by mass spectrometry. Therefore, the following
122 decomposition is proposed [30].



127 As a starting point for considering the mechanism of the reaction given by reaction (2), it
128 was accepted that the thermal decomposition process of this reaction could be either a
129 chemical reaction on the FeS₂/FeS interface, or the diffusion of sulfur vapor through the layer
130 of FeS (pyrrhotite) [31]. It is also reported by Zivkovic et al. [32] that sulfur vapor appears in
131 the pyrrhotite produced at a lower temperature (440-500 °C). Compared with the
132 decomposition of pure pyrite in nitrogen, the initial decomposition temperature of the
133 coal-derived pyrite/marcasite is nearly lower by 100 °C [29, 18, 28]. It suggests that the

134 indigenous hydrocarbon with hydrogen donor ability in coal can promote the reduction of
135 pyrite/marcasite, though the overall deficit of hydrogen makes the thermal decomposition
136 reaction of pyrite/marcasite to prevail in pyrolysis [11]. It was reported that the decomposition
137 of pyrite to pyrrhotite follows the unreacted core model [28, 10]. Therefore, the reaction (2)
138 should be considered in thermal decomposition process without oxygen for the inner portion
139 of pyrite particles.

140 It was stated both by Paulik et al. [33, 28] and Shkodin et al. [29] that three endothermic
141 effects are observed in the thermoanalytical curves of pyrite: at 450-480 °C, 530-570 °C and
142 630-690 °C successively. The first endothermic effect in the thermoanalytical curves of pyrite
143 in an inert gas stream at atmospheric pressure appears to be connected with the elimination of
144 gaseous liquid inclusions. The second endothermic effect at 530-570 °C is interpreted as the
145 decomposition process of the iron oxide sulfate film on the surface of the mineral and
146 subsequent dissociation of pyrite, involving the removal of disulfide sulfur on its surface and
147 formation of pyrrhotite on the freshly-formed surface. The third effect is related to the
148 dissociation of pyrite in its total bulk, yielding pyrrhotite and subsequently also troilite. The
149 transformations at 450-480 °C and 530-570 °C, however, are interpreted differently by
150 different researchers. Some authors [3] assume that the effect at 530-570 °C has no
151 connection with the dissociation of pyrite, while data of other authors [4] indicate that pyrite
152 partially dissociates, yielding pyrrhotite. According to Berg and co-workers [2] the
153 endothermic effect at 450-480 °C is caused by evolved impurities and gaseous or liquid
154 inclusions, and also by defects in the crystal lattice. The thermal process at 530-570 °C is
155 attributed by these authors to the evolution of oxidized "non-equivalent" sulfur located on the

156 surface of the pyrite. Simultaneously they observed an increase in magnetic susceptibility, due
157 to the appearance of pyrrhotite.

158

159 *Mass spectrometric analysis of the evolved gases*

160 The evolved products during the thermal decomposition of the coal-derived
161 pyrite/marcasite were determined by thermogravimetry coupled to a mass spectrometer and
162 are shown in Fig.3. The interpretation of the mass spectra occurs on the basis of degassing
163 profiles from the molecule ions of water vapor (H_2O : $m/Z=18$), carbon dioxide (CO_2 :
164 $m/Z=44$), sulfur dioxide (SO_2 : $m/Z=64$) as well as by fragment ions (OH^+ : $m/Z=17$, O^+ :
165 $m/Z=16$, $^{32}\text{S}^+$: $m/Z=32$; $^{34}\text{S}^+$: $m/Z=34$, SO^+ : $m/Z=48$).

166 Combined with the TG-DTG analysis curves, six thermal decomposition steps are
167 observed. The first step at 116 °C is due to loss of the adsorbed water molecules on the
168 external surfaces of the mineral particles. The characterization of water release by means of
169 MS is possible with the molecule ion H_2O^+ ($m/Z=18$) together with the fragment ion OH^+
170 ($m/Z=17$) and O^+ ($m/Z=16$). Peak at 148 °C for the sample is found in the ion current curve
171 for H_2O^+ ($m/Z=18$); corresponding peaks are also found in the ion current curves for OH^+
172 ($m/Z=17$) and O^+ ($m/Z=16$). It can be safely concluded that water is given out at about 148 °C
173 for the sample, which is consistent with the mass loss observed at about 148 °C from the TG
174 curves. The third step at 251 °C is assigned to the evolution of sulfur on the pyrite surface and
175 loss of the rest part of interparticle water. This result is good agreement with the results of
176 Thomas et al. [18]. The last three assignments are based on the MS data shown in Fig.3. Peaks
177 at 501, 548 and 598 °C for the sample are found in the ion current curve for SO_2^+ ($m/Z=64$);

178 corresponding peaks are also found in the ion current curves for SO^+ ($m/Z=48$), ^{34}S ($m/Z=34$)
179 and $^{32}\text{S}^+$ ($m/Z=32$). The evolution profiles of the ions at $m/Z=64$ (SO_2^+) and $m/Z=48$ (SO^+)
180 the fragment ion are used to identify the presence of SO_2 . The $m/Z=64$ and 48 peaks observed
181 to follow the TG-DTG peaks indicating the evolution SO_2 during both steps of the thermal
182 decomposition. It is observed that the final product of the decomposition, as determined from
183 XRD, was hematite (Fe_2O_3) which is in agreement with the previous literature [18]. It is also
184 reported by Jorgensen and Moyle [34] that hematite (Fe_2O_3) is the solid end product of the
185 reaction in this temperature range. They further concluded that small amounts of pyrrhotite
186 formed as thin layers of intermediate reaction product but in amounts which are small in
187 comparison with the amount of hematite. Thus, Eq. (4) is a reasonable candidate for this
188 process. It is also indicated that the chemical substance SO_2 is present in the thermal
189 decomposition for the sample, and this will be further proved by the following IR results.

190 The three broad peaks at 501, 548 and 598 °C is found in the ion current curve for CO_2
191 ($m/Z=44$). This illustrate a small proportion of CO_2 is given out in this temperature range.
192 This may be due to the pyrolysis of the residual coal. It is also observed that the relative
193 intensity of CO_2 increase as temperature goes up. The MS data, using $m/Z=80$ curve, for this
194 decomposition process indicated that no SO_3 was produced.

195 It is interesting to note that the three temperature peaks occurred one after another and
196 the corresponding temperature range overlap each other during thermal decomposition
197 process. This phenomenon suggests that coal-derived pyrite/marcasite undergo the
198 decomposition till 650 °C and different transition states appeared one after another during the
199 decomposition. Clearly, there are at least three transition state structures with different Fe/S

200 values during thermal decomposition, which corresponds with the temperature peaks on MS
201 profile. It should be noted that SO_3 was not observed as a product as no peak was observed in
202 the $m/Z=80$ curve. It has been reported that mineral pyrite is slightly different from coal pyrite
203 in reactivity due to their surface structure and morphology [35, 3]. The investigation by
204 Sundaram [35] revealed that oxidation rate of coal pyrite was twice as high as that of mineral
205 pyrite at 5% oxygen; and four times as high as that of mineral pyrite at 10% oxygen.
206 Therefore, compared with the decomposition of pure pyrite, the initial decomposition
207 temperature of the coal-derived pyrite/marcasite is nearly lower by 100 °C [29, 18, 28, 36,
208 37].

209 According to experimental results of the mass spectrometric analysis, the gaseous
210 species produced by the thermal decomposition using the mass spectra made evident the
211 following:

- 212 a) The evolved products at 116, 148 °C: water;
- 213 b) The evolved products at 251 °C: sulfur vapor and water;
- 214 c) The evolved products at 501, 548 and 598 °C: sulfur dioxide, carbon dioxide and
215 water;

216 Based on these results, it can be concluded that the thermal decomposition of pyrite to
217 pyrrhotite follows the unreacted core model between 450-520 °C. Pyrite can be oxidized
218 directly or oxidized after it is firstly decomposed into pyrrhotite and sulfur. Hematite (Fe_2O_3)
219 is the solid end product of the reaction in the temperature range of 550-650 °C, and SO_3 was
220 not observed as a product for the thermal decomposition of the coal-derived pyrite/marcasite.
221 It is indicated that the chemical substance SO_2 is present as the main gaseous product in the
222 thermal decomposition for the sample. The coal-derived pyrite/marcasite is different from

223 mineral pyrite in reactivity due to their surface structure and morphology.

224

225 *Infrared spectroscopy analysis of the evolved gases*

226 Fig.4 shows 3D FTIR spectra for the gases produced from the thermal decomposition of
227 the coal-derived pyrite/marcasite. By comparing the spectra over the range 30-800 °C, it is
228 important to note that the spectra not only provide the information about the species of the
229 released gas, but also display the relative intensities of the evolved gas. It can be observed
230 from the spectra that the pyrolysis products for the sample mainly vary in amounts but not in
231 species. Combined with the mass spectroscopic analysis, main products are identified as
232 follows: water (H₂O), carbon dioxide (CO₂), and sulfur dioxide (SO₂). The emission of sulfur
233 dioxide (SO₂) is confirmed by the appearance of absorption bands in the range 1300-1450
234 cm⁻¹ and 1150 cm⁻¹. The characteristic bands of CO₂ at 2217-2391 cm⁻¹ indicate its formation.
235 The emission of water follows three steps. At low temperature, the absorbed water is released
236 out by evaporation. Moreover, when the temperature reaches 150 °C, water was generated by
237 the loss of interparticle water for the sample. In addition, an amount of water released out
238 according to the characteristic band at 3500-3850 cm⁻¹.

239 FT-IR spectra of thermal decomposition products of the coal-derived pyrite/marcasite at
240 different temperature are shown in Fig. 5. As the temperature of the system is raised, the
241 emission of water (H₂O) mainly occurred between 100 and 200 °C, and this temperature
242 range of mass loss is attributed to the loss of absorbed water for the sample. At the same time,
243 the sulfur dioxide (SO₂) is still detected by the *in situ* FTIR spectroscopic evolved gas
244 analysis. The evolved process within 450-650 °C can be divided into three parts: the first

245 evolved process for the SO₂ with the maximum rate at 500 °C, and this temperature range of
246 losing these two types of products is assigned to the oxidation of the sample particle surface
247 and the decomposition of the interior for the pyrite particle without oxygen; the second
248 evolved process for the SO₂ with a maximum at 550 °C is due to the evolution of oxidized
249 sulfur stemmed from the last step the decomposed of the pyrite particle without oxygen, Eq.
250 (3); the third evolved process for the SO₂ with a maximum at 600 °C is attributed to the
251 oxidation of the pyrrhotite, Eq.(4). According to the report by Hong and Fegley [36], no
252 hematite (Fe₂O₃) but only pyrrhotite was observed within the temperature range of
253 400-520 °C. Paulik et al. [28] found that Eq. (2) should be considered in thermal
254 decomposition process without oxygen for the inner portion of pyrite particles. Therefore, it is
255 concluded that the mass loss at 450-521 °C is caused by the oxidation of the sample particle
256 surface and the decomposition of the interior for the pyrite particle without oxygen, in
257 accordance with Eq. (1) and Eq. (2). A conclusion can be drawn that the mass loss in this
258 stage is mainly caused by the release of SO₂, with the unique existence of characteristic bands
259 at 1300-1450 cm⁻¹ and 1150 cm⁻¹. It is also observed that a small amount of the CO₂ and the
260 water are release in this temperature range. The absorption bands of volatile for the sample
261 also appear to be at the same wavenumbers, while the diversities of the absorbance only exist
262 in 1300-1450 cm⁻¹ region. The release of water and CO₂ (bands at 3500-3850 and 2217-2391
263 cm⁻¹ region) is less violent, while the relative intensity of SO₂ firstly increases and then
264 decreases. It is reported that pyrrhotite is an intermediate phase produced during heating of
265 pyrite [38]. The researchers further proposed that hematite is the major reaction product
266 during heating pyrite in a restrictive oxidative environment. Thus Eq. (4) is a reasonable

267 candidate for the last decomposition process.

268 Based on the results of this study and through reviewing and summarizing various study
269 results, it can be concluded that the coal-derived pyrite/marcasite first decomposed to form
270 pyrrhotite. The formed pyrrhotite was then oxidized to form oxides. The analysis showed the
271 existence of pyrite, marcasite, pyrrhotite and hematite at the later stage of the roasting process.
272 This is an indication of the occurrence of simultaneous thermal decomposition of the pyrite
273 and the oxidation of the formed pyrrhotite.

274

275 **Conclusions**

276 The products evolved during the thermal decomposition of the coal-derived
277 pyrite/marcasite were studied by using TG-FTIR-MS technique. The main mass losses for the
278 thermal decomposition of the coal-derived pyrite/marcasite were observed at 116, 148, 251,
279 501, 548 and 598 °C which were attributed to (a) loss of the adsorbed water (b) the loss of
280 interparticle water for the sample (c) the evolution of sulfur on the pyrite surface and loss of
281 the rest part of interparticle water (d) the oxidation of the sample particle surface and the
282 decomposition of the interior for the pyrite particle without oxygen (e) the evolution of
283 oxidized sulfur stemmed from the last step the decomposed of the pyrite particle without
284 oxygen and (f) the oxidation of the pyrrhotite. These thermal decomposition processes and
285 products were proved by the mass spectrometric analysis and infrared spectroscopic analysis
286 of the evolved gases.

287 The main gases and volatile products released during the thermal decomposition of the
288 coal-derived pyrite/marcasite are water vapor (H₂O), carbon dioxide (CO₂), sulfur dioxide

289 (SO₂). The evolved products obtained were mainly divided into two processes: 1) the main
290 evolved product H₂O is mainly released at below 300 °C; 2) under the temperature of
291 450-650 °C, the main evolved products are SO₂ and small amount of CO₂. It should be noted
292 that SO₃ was not observed as a product as no peak was observed in the m/Z=80 curve. The
293 oxidation of the coal-derived pyrite/marcasite starts at about 450 °C and that pyrrhotite and
294 hematite are formed as primary products. The chemical substance SO₂ is present as the main
295 gaseous product in the thermal decomposition process for the sample. The coal-derived
296 pyrite/marcasite is vastly different from mineral pyrite in thermal decomposition temperature
297 due to their surface structure and morphology. The mass spectrometric analysis results are in
298 good agreement with the infrared spectroscopic analysis the evolved gases. Thermal analysis
299 and mass spectrometric analysis clearly show at which temperature the mass loss. However,
300 infrared spectroscopic analysis will give the evidence on the thermal decomposition products.
301 These results make all explanation have the sufficient evidence. Therefore, thermal analysis
302 coupled with spectroscopic gas analysis is demonstrated to be a powerful tool for the
303 investigation of gas evolution from the thermal decomposition of materials and its
304 intercalation complexes. Using different gas analyzing methods like MS and FTIR increases
305 the unambiguous interpretation of the results.

306

307 **Acknowledgments**

308 The authors gratefully acknowledge the financial support provided by the National Natural Science Foundation
309 of China (No. 51034006) and the Open Research Project of State Key Laboratory for Coal Resources and Safe
310 Mining, China University of Mining & Technology (SKLCRSM11KFB06).

References

1. Hu H, Chen Q, Yin Z, Zhang P. Thermal behaviors of mechanically activated pyrites by thermogravimetry (TG). *Thermochim Acta*. 2003;398:233-40.
2. Boyabat N, Özer AK, Bayrakçeken S, Gülaboğlu MS. Thermal decomposition of pyrite in the nitrogen atmosphere. *Fuel Process Technol*. 2004;85:179-88.
3. Bylina IV, Mojumdar SC, Papangelakis VG. Effect of storage time on the pressure oxidation enthalpy of pyrite. *J Therm Anal Calorim*. 2012;108:829-35.
4. Iliyas A, Hawboldt K, Khan F. Kinetics and safety analysis of sulfide mineral self-heating. *J Therm Anal Calorim*. 2011;106:53-61.
5. Gryglewicz G, Wilk P, Yperman J, Franco DV, Maes II, Mullens J, Van Poucke LC. Interaction of the organic matrix with pyrite during pyrolysis of a high-sulfur bituminous coal. *Fuel*. 1996;75:1499-504.
6. Kaljuvee T, Keelman M, Trikkel A, Petkova V. TG-FTIR/MS analysis of thermal and kinetic characteristics of some coal samples. *J Therm Anal Calorim*. 2013;113:1063-71.
7. Babiński P, Łabojko G, Kotyczka-Morańska M, Plis A. Kinetics of coal and char oxycombustion studied by tg-ftir. *J Therm Anal Calorim*. 2013;113:371-8.
8. Cui X, Zhang X, Yang M, Feng Y, Gao H, Luo W. Study on the structure and reactivity of corex coal. *J Therm Anal Calorim*. 2013;113:693-701.
9. Liu Z, Zhang Y, Zhong L, Orndroff W, Zhao H, Cao Y, Zhang K, Pan W-P. Synergistic effects of mineral matter on the combustion of coal blended with biomass. *J Therm Anal Calorim*. 2013;113:489-96.
10. Hu G, Dam-Johansen K, Wedel S, Hansen JP. Decomposition and oxidation of pyrite. *Prog Energy Combust*. 2006;32:295-314.
11. Chen H, Li B, Zhang B. Decomposition of pyrite and the interaction of pyrite with coal organic matrix in pyrolysis and hydrolysis. *Fuel*. 2000;79:1627-31.
12. Yan J, Xu L, Yang J. A study on the thermal decomposition of coal-derived pyrite. *J Anal Appl Pyrol*. 2008;82:229-34.
13. Murphy R, Strongin DR. Surface reactivity of pyrite and related sulfides. *Surf Sci Rep*. 2009;64:1-45.
14. Zhang X, Borda MJ, Schoonen MAA, Strongin DR. Adsorption of phospholipids on pyrite and their effect on surface oxidation. *Langmuir*. 2003;19:8787-92.
15. Eneroth E, Koch CB. Crystallite size of haematite from thermal oxidation of pyrite and marcasite—effects of grain size and iron disulphide polymorph. *Miner Eng*. 2003;16:1257-67.
16. Sit PHL, Cohen MH, Selloni A. Interaction of oxygen and water with the (100) surface of pyrite: Mechanism of sulfur oxidation. *J Phys Chem Lett*. 2012;3:2409-14.
17. Hansen JP, Jensen LS, Wedel S, Dam-Johansen K. Decomposition and oxidation of pyrite in a fixed-bed reactor. *Ind Eng Chem Res*. 2003;42:4290-5.
18. Thomas P, Hirschausen D, White R, Guerbois J, Ray A. Characterisation of the oxidation products of pyrite by thermogravimetric and evolved gas analysis. *J Therm Anal Calorim*. 2003;72:769-76.
19. Ahamad T, Alshehri SM. TG-FTIR-MS (evolved gas analysis) of bidi tobacco powder during combustion and pyrolysis. *J Hazard Mater*. 2012;199–200:200-8.
20. Madarász J, Brăileanu A, Crişan M, Pokol G. Comprehensive evolved gas analysis (EGA) of amorphous precursors for s-doped titania by in situ TG-FTIR and TG/DTA-MS in air: Part 2.

- Precursor from thiourea and titanium(iv)-n-butoxide. *J Anal Appl Pyrol.* 2009;85:549-56.
21. Madarász J, Varga PP, Pokol G. Evolved gas analyses (TG/DTA-MS and TG-FTIR) on dehydration and pyrolysis of magnesium nitrate hexahydrate in air and nitrogen. *J Anal Appl Pyrol.* 2007;79:475-8.
 22. Madarász J, Pokol G. Comparative evolved gas analyses on thermal degradation of thiourea by coupled tg-ftir and tg/dta-ms instruments. *J Therm Anal Calorim.* 2007;88:329-36.
 23. Fischer M, Wohlfahrt S, Saraji-Bozorgzad M, Matuschek G, Post E, Denner T, Streibel T, Zimmermann R. Thermal analysis/evolved gas analysis using single photon ionization. *J Therm Anal Calorim.* 2013;113:1667-73.
 24. Arockiasamy A, Toghiani H, Oglesby D, Horstemeyer MF, Bouvard JL, King R. TG-DSC-FTIR-MS study of gaseous compounds evolved during thermal decomposition of styrene-butadiene rubber. *J Therm Anal Calorim.* 2013;111:535-42.
 25. Bednarek P, Szafran M. Thermal decomposition of monosaccharides derivatives applied in ceramic gelcasting process investigated by the coupled DTA/TG/MS analysis. *J Therm Anal Calorim.* 2012;109:773-82.
 26. Qian XF, Zhang XM, Wang C, Tang KB, Xie Y, Qian YT. Solvent-thermal preparation of nanocrystalline pyrite cobalt disulfide. *J Alloy Compd.* 1998;278:110-2.
 27. Lawson RT. Aqueous oxidation of pyrite by molecular oxygen. *Chem Rev.* 1993;82:461-97.
 28. Paulik F, Paulik J, Arnold M. Kinetics and mechanism of the decomposition of pyrite under conventional and quasi-isothermal — quasi-isobaric thermoanalytical conditions. *J Therm Anal Calorim.* 1982;25:313-25.
 29. Shkodin VG, Abishev DN, Kobzhasov AK, Malyshev VP, Mangutova RF. The question of thermal decomposition of pyrite. *J Therm Anal Calorim.* 1978;13:49-53.
 30. Cheng H, Liu Q, Huang M, Zhang S, Frost RL. Application of TG-FTIR to study SO₂ evolved during the thermal decomposition of coal-derived pyrite. *Thermochim Acta.* 2013;555:1-6.
 31. Jovanović D. Kinetics of thermal decomposition of pyrite in an inert atmosphere. *J Therm Anal Calorim.* 1989;35:1483-92.
 32. Zivkovic ZD, Mitevska N, Savovic V. Kinetics and mechanism of the chalcopyrite-pyrite concentrate oxidation process. *Thermochim Acta.* 1996;282-283:121-30.
 33. Paulik J, Paulik F, Arnold M. Simultaneous TG, DTG, DTA and EGA technique for the determination of carbonate, sulphate, pyrite and organic material in minerals, soils and rocks. *J Therm Anal Calorim.* 1982;25:327-40.
 34. Jorgensen FRA, Moyle FJ. Gas diffusion during the thermal analysis of pyrite. *J Therm Anal Calorim.* 1986;31:145-56.
 35. Sundaram HP, Cho EH, Miller A. SO₂ removal by leaching coal pyrite. *Energ Fuel.* 2001;15:470-6.
 36. Hong Y, Fegley B. The kinetics and mechanism of pyrite thermal decomposition. *Berichte der Bunsengesellschaft für physikalische Chemie.* 1997;101:1870-81.
 37. Cleyle PJ, Caley WF, Stewart L, whiteway SG. Decomposition of pyrite and trapping of sulphur in a coal matrix during pyrolysis of coal. *Fuel.* 1984;63:1579-82.
 38. Bhargava SK, Garg A, Subasinghe ND. In situ high-temperature phase transformation studies on pyrite. *Fuel.* 2009;88:988-93.

LIST OF TABLES

Table 1 The minerals composition of the coal-derived pyrite/marcasite sample

Table 1 The minerals composition of the coal-derived pyrite/marcasite used in this experiment

Mineral	Pyrite	Marcasite
Content of mineral /mass%	46.9	53.1

LIST OF FIGURES

Fig. 1. XRD pattern for the coal-derived pyrite/marcasite

Fig. 2. TG-DTG curves of the coal-derived pyrite/marcasite

Fig. 3. Mass spectrometric analysis of the evolved gases for the coal-derived pyrite/marcasite

Fig. 4. 3D FTIR spectra of the evolved gases for the coal-derived pyrite/marcasite

Fig.5. Infrared spectroscopy analysis of the evolved gases for the coal-derived pyrite/marcasite

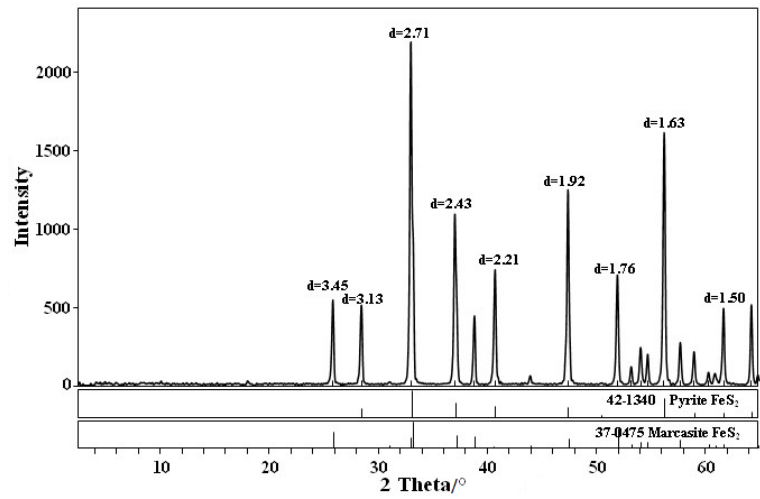


Fig.1

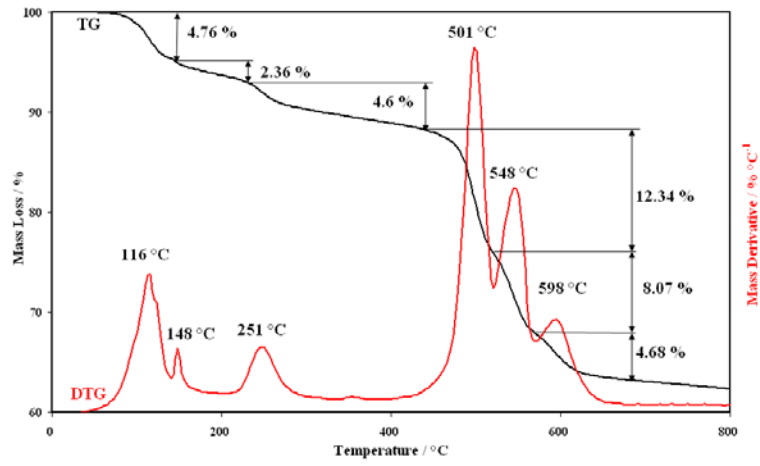


Fig.2

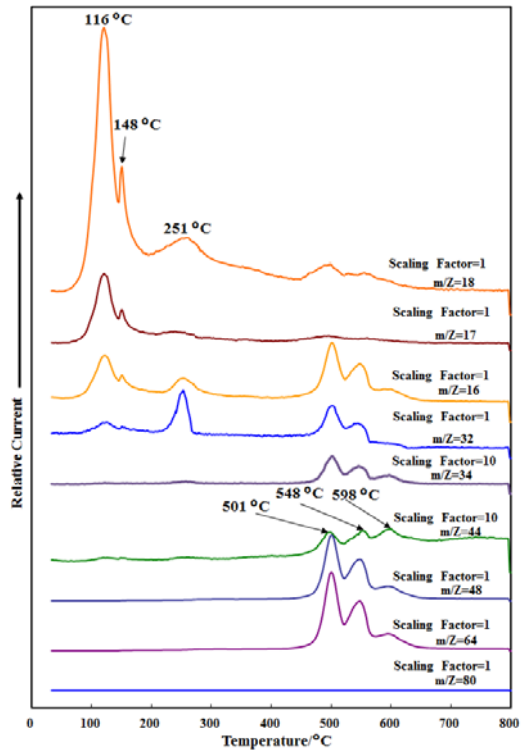


Fig.3

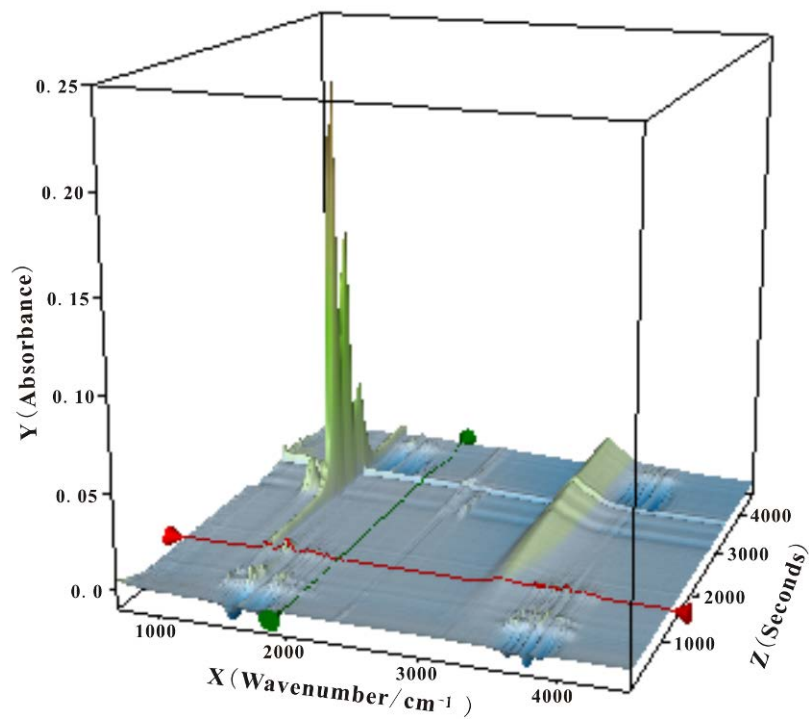


Fig.4

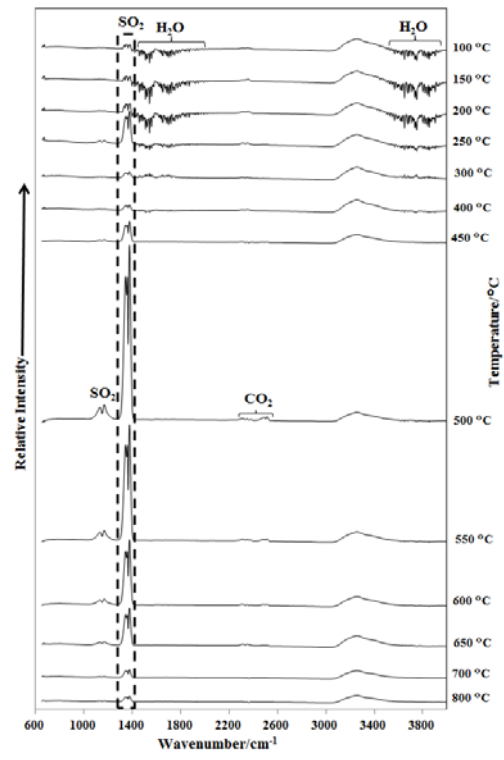


Fig.5